

MONITORING AND SIMULATING HUMIDITY PROFILES IN CONCRETE ELEMENTS DURING DRYING

Miguel Azenha ⁽¹⁾, José Granja ⁽¹⁾

(1) University of Minho, Guimarães, Portugal

Abstract

Integrated approaches towards the measurement and simulation of the internal humidity of cement based materials, in which the same team accomplishes all the tasks are scarce in the literature. Furthermore, the measurement of humidity in cement-based materials is a subject that requires experience and significant care to obtain reliable data. In view of this reasoning, the research here reported pertains to an integrated approach that focuses in two main topics: (a) several issues regarding the experimental measurement of internal humidity in cement based materials through sleeved humidity probes, with test series devoted to each issue (namely the type of sensor, the existence of Gore Tex fabric to protect the sensor and the influence of the permanence time of probes within measuring sleeves); (b) an experimental program for humidity measurement in concrete specimens, followed by the simulation through the formulation forwarded in the MC1990/2010. The successful achievement of the measurements and simulations reported herein corroborate the validity of the adopted strategies and assumptions.

1 Introduction

The serviceability of concrete structures is strongly affected by shrinkage phenomena, which in turn are conditioned by internal moisture [1]. An adequate assessment of internal stress states in concrete structures during service demands for a proper knowledge of internal moisture distributions and the corresponding volumetric changes.

When non-destructive testing is chosen, the most usual method of measurement consists in embedding relative humidity probes into concrete [2-4]. This measuring strategy brings about experimental difficulties due to several reasons. Furthermore, few research works exist that actually combine the experimental assessment and corresponding numerical simulation of

humidity in concrete, with the ultimate objective of simulating concrete stresses due to shrinkage.

This paper focuses on the description of an experimental and simulation program targeted to humidity profiling in concrete prismatic specimens. The first part of the research is devoted to several experimental issues in humidity profiling, leading to a reliable set of procedures for such end. Then, in a second part, a description of an experimental program with three prismatic of distinct sizes is shown. Finally, a simulation through the finite difference method is shown, highlighting the possibility of adopting a single set of simulation parameters that successfully describe the behaviour of all specimens.

2 Humidity measurement issues

Given the scarcity of works in the literature regarding comparative studies of hygrometric methods for monitoring moisture in concrete [4], a series of laboratory tests was devised for better understanding the limitations and possibilities associated to the humidity profiling in cement-based materials. The tests reported here involve the use of relative humidity (RH) sensors embedded into a specimen made of cement based materials (e.g. concrete, mortar or cement paste). The embedment process is ensured by a 'cast-in' sleeve that allows the RH sensor to come into direct contact with the region of interest to be monitored. The space within the sleeve where the sensor stays during measurement is fully sealed, except for the extremity in which the measurement is desired. The humidity sensor ends up measuring the humidity in the macro-pore (void) that is formed by the sleeve, which is considered to be in equilibrium with the average pore humidity of its extremity in contact with the measurement surface. The following issues were addressed in concern to such testing technique: (i) the relative performance of several available systems for measuring RH; (ii) the influence of using Gore-Tex[®] as a protective interface between the measuring sleeve and the material under testing; and (iii) the possible disrupting effect of having inclusion/removal cycles of the sensors inside the measurement sleeves.

2.1 Performance of the RH measurement systems

A systematic experimental study was carried out in order to assess the performance of various types of sensors under conditions that are equivalent to their use for measuring the internal RH of concrete (i.e., within an embedded macro-pore). The comparative program consisted in placing each sensor to be tested within a PVC tube with a 15 mm diameter and 70 mm length, as shown in Figure 1a. One extremity of the tube was sealed with several overlapping layers of plastic tape (technique that showed positive results in previous experiments), whereas the opposite end was covered with a 3 mm thick disk of fresh cement paste (CEM I 42.5R, with w/c=0.5), with a diameter equal to the interior one of the PVC tube. During the execution of the cement paste disks, special attention was addressed to controlling their thicknesses. Despite this fact, at the end of the test the thickness of each disk was measured, and a variation of ± 0.30 mm ($\pm 10\%$) in regard to the target value was observed. The discs had however a perfectly cylindrical shape, with no gaps between the PVC wall and the cement paste. During the first 68 h of testing the cement paste was kept in sealed conditions on the bottom of the tube, through the use of a plastic tape. After 68 h of curing the plastic tape was

removed, promoting drying of the cement paste towards the environment (see Figure 1a). At this stage the samples were placed inside a container ($22.8 \times 13.2 \times 10.7 \text{ cm}^3$) with a NaCl salt solution, allowing therefore the creation of an environment with $\text{RH} = 75\%$ ($T = 20 \text{ }^\circ\text{C}$) (see Figure 1b). This test was conducted on four specimens, each containing one of the types of sensor being studied, with the following designations: VS 7 (Vaisala HM44 [5]), PR-7 (Proceq Hygropin [6]), SHT-7 (Sensirion SHT75 [7]) and HW-7 (Honeywell HIH4000 [8]).

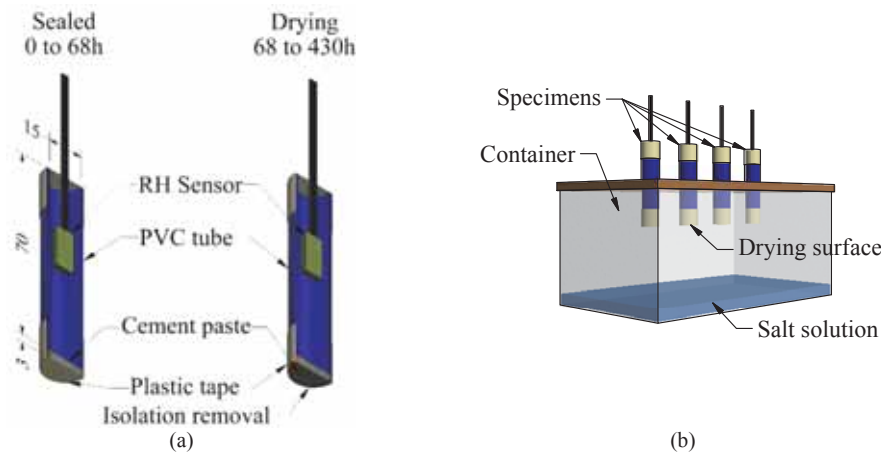


Figure 1: (a) Scheme of the specimens; (b) Ongoing test in the drying phase ($\text{RH}=75\%$) [units: mm].

The results of this experimental program are shown in Figure 2. Despite some problems in the first 3 days due to failures of the data acquisition equipment problems, a good coherence of the RH measurements is confirmed: the sensors behaved as expected during the first 68 h, with a measured RH close to 100% in correspondence to the effective sealing of the tube, and low self-desiccation of the cement paste (high w/c ratio). It can be observed that a very good coherence was obtained between the different sensors at the end of the test (18 days), with RH deviations smaller than $\pm 2.5\%$. The monotonic decreasing trend of the humidity between 3 and 18 days is also quite similar in several sensors, exhibiting however somewhat more relevant differences between the ages of 4 and 6 days. It should be noted that such dispersion of results has been reported as well by other authors [9]. It is worth noting that when the humidity sensors are exposed for long periods to very high RH (above 95%), they may undergo decalibration and/or a delay in the measurements when the air humidity returns to lower values [10]. The latter situation can be identified in Figure 2 for sensor PR-7, which underwent a delay of $\sim 1.6 \text{ h}$ (point (1)) right after removal of the cement paste surface insulation, and almost 1 day during the drying phase (zone (2)).

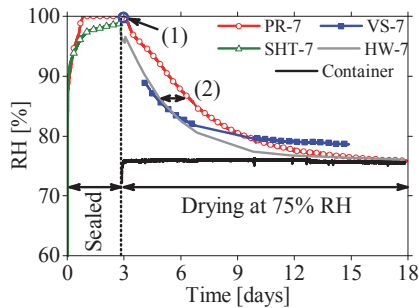


Figure 2: Test results concerning the behaviour of the sensors in the macro-pore.

2.2 Influence of using Gore-Tex® to protect the sensors

When the macro-pore to host the RH sensor is materialized by a pre-placed sleeve in concrete, into which the RH sensor is embedded since casting, it is necessary to avoid filling of the sleeve with fresh cement paste and to protect the sensor from liquid damage (same situation with mortar or concrete). However, this macro-pore needs to contact with the surrounding material, in order to allow a vapour exchange between the cementitious material and the air inside the pore. In several works of Grasley et al. [4, 11] a Gore-Tex® fabric [12] was used as an interface between the macro-pore and the material during casting. However, given the lack of studies regarding the influence that this interface material can have on the accuracy of concrete RH measurements in embedded macro-pores. For this purpose, two types of Gore-Tex® fabric were studied which have different water vapour resistances: Civil Gore-Tex® (GT1) (Water vapour resistance of 9 s/m) and Military Gore-Tex® (GT2) (Water vapour resistance of 13 s/m).

The principle of the test is very similar to that explained in the previous section, differing only in the dimensions of the PVC tube (with a length of 40 mm, in this case) and the inclusion of a Gore-Tex® fabric between the cement paste and the internal air of the macro-pore. In this test, only SHT and HW sensors were used. In all remaining aspects (environmental conditions and experimental procedure) this test is identical to the one described in Section 2.1 – see Figure 3a. Four samples were tested: two without Gore-Tex® (HW-4 and SHT-4), one with Civil Gore-Tex® (HW 4 GT1) and one with Military Gore-Tex® (HW-4 GT2). By observing the collected results in Figure 3b, it can be noticed that the inclusion of Gore-Tex® fabrics in the interface between the macro-pore and cement paste had no significant effect, irrespective to its type (Civil or Military). In fact, the level of scattering obtained for these results is in all aspects similar to the one reported in Figure 2 of Section 2.1

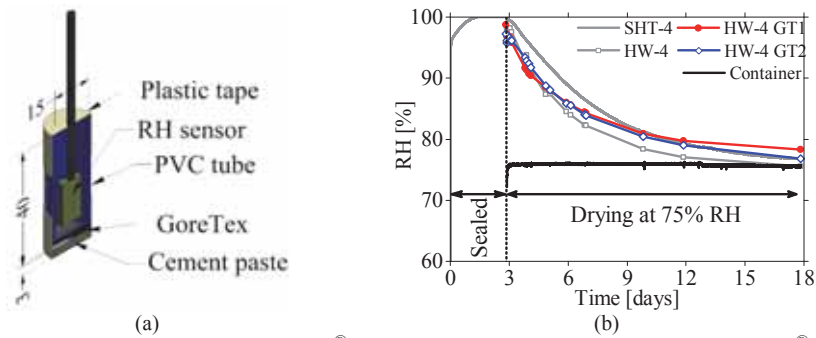


Figure 3: (a) Test scheme with Gore-Tex® [units: mm]; (b) test results with Gore-Tex®.

2.3 Use of permanently installed sensors vs discrete monitoring

A potentially criticisable aspect of the commercial integrated systems for RH measurement analysed in the context of this work concerns to the possible moisture exchanges between the measuring sleeve and the surrounding environment when the RH sensor is being installed or removed (the case of VS and PR probes). To assess this issue, an additional experiment was performed using two Vaisala systems in two $5 \times 5 \times 5 \text{ cm}^3$ mortar specimens, according to the scheme reproduced in Figure 4a. The composition of the mortar expressed per m^3 was: 280 kg of CEM I 42.5R; 143 kg of water; 40 kg of fly-ash; 6.25 kg of super-plasticizer; 245.6 kg of sand (0/4).

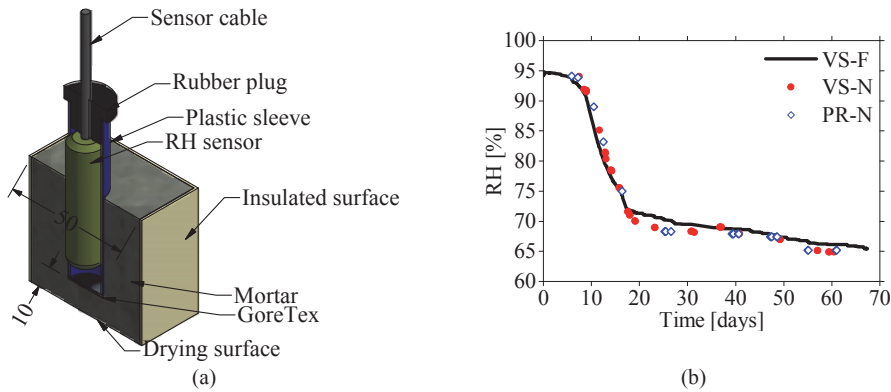


Figure 4: (a) Specimen used in the test [units: mm]; (b) Test results for evaluating the influence on RH measurements of macro-pore access at discrete instants.

Both systems were used with the plastic sleeve provided by the manufacturer (with 16 mm diameter and 70 mm long). To accelerate the drying process, the measuring extremity of the sleeve was positioned 10 mm away from the drying surface (see Figure 5a). Military Gore-Tex® was placed to prevent the entry of cement paste into the tube during casting.

The samples were kept in sealed conditions during the first 7 days of curing at 20 °C. Afterwards, the two surfaces of the specimen that are perpendicular to the axis of the plastic sleeve were exposed to drying. The other four surfaces of the specimen were sealed with paraffin, ensuring a unidirectional moisture flow. During the drying period specimens were kept under controlled temperature and RH ($T = 20\text{ °C}$ and $RH = 60\%$) inside a climatic chamber. One of the sensors was used according to the manufacturer instructions: placement and removal of the sensor in the macro-pore for each measurement (VS-N). The other sensor was permanently placed inside the macro-pore, which remained sealed throughout the entire experiment (VS-F). Additionally, in the specimen where discrete measurements were performed, two different sensors were used: a Proceq sensor (PR-N), intercalated with the above mentioned VS-N sensor. Results collected since the instant of exposure to drying until the end of the experiment, 2.5 months later, are shown in Figure 4b. It can be observed that the measurements recorded by the two different methods were identical in all analysed instances.

3 Humidity profiling: experiments and simulation

3.1 Materials

A single batch of concrete has been studied in the scope of this work, with the following mix composition per m^3 : 280 kg of CEM II 42.5R; 40 kg of fly ash; 143 kg of water; 6 kg of water reducing admixture; 786 kg of medium sand (river); 245 kg of fine sand; 417 kg of gravel 6/14; and 478 kg of gravel 14/20. The mixing procedures followed the recommendations of [13].

3.2 Humidity profiles in concrete specimens

The humidity profiles in the concrete prisms were assessed through the embedment of humidity sensors within cast-in sleeves within concrete. Three specimen geometries were considered, $10 \times 10 \times 40\text{ cm}^3$, $15 \times 15 \times 60\text{ cm}^3$ and $20 \times 20 \times 60\text{ cm}^3$, with the designations of S10, S15 and S20, respectively (a single specimen per each size). All specimens were cast into plywood moulds (see Figure 5) with pre-embedded sleeves that allowed access to measurement points at predefined depths for humidity profiling. Each sleeve had external/internal diameters of 16/13.6 mm, and a specially designed cap to maintain its free extremity (i.e., outside the specimen) sealed both during and in-between measurements. The extremity of the sleeve that was embedded into concrete was protected with the Military Gore-Tex[®].

The specimens were cast and permanently kept in a climatic chamber with temperature $T = 20 \pm 0.5\text{ °C}$ and $RH = 60 \pm 1.5\%$. Right after casting, plastic films were placed over the free surface of concrete, thus ensuring adequate sealing. The specimens were then left undisturbed until the age of 7 days. At such age, the plywood forms and board were removed, and four of the surfaces of each specimen were sealed with several layers of paraffin wax ($>2\text{ mm}$ thick), according to the schematic view of Figure 5c. The two surfaces that were left unsealed ensure that the drying flow on the specimen is 1D and follows the direction of the embedded sleeves. It is however remarked that the sensing extremities of the sleeves were always placed in such a location that each sleeve did not disturb the path for moisture movement between the

measuring point and the nearest drying surface, as shown in Figure 5a. The depths at which internal concrete RH measurements were taken are shown in Figure 5d.

The measurement of humidity within the sleeves was performed with a Vaisala HM44 probe. The probes were inserted at selected instants, with each point of measurement being assessed according to the observed evolution, maintaining however a maximum interval of 2 weeks between consecutive measurements.

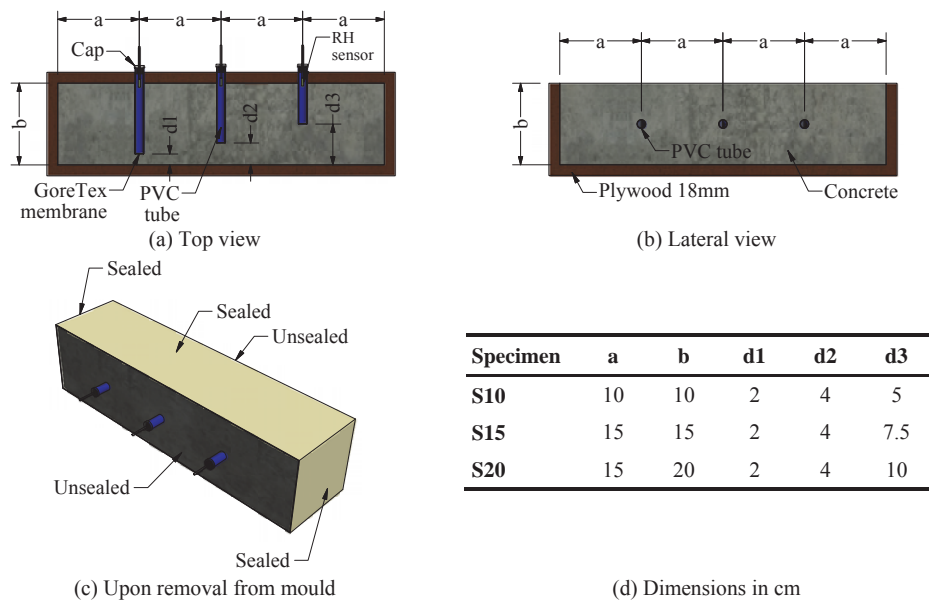


Figure 5: Schematic representation of the specimens for humidity profiling: (a) top view; (b) lateral view; (c) perspective after removal and sealing (i.e. under testing); (d) table with specimens' dimensions and measurement depths [units: cm].

The measurement results for the three sizes of specimens studied (S10, S15 and S20) are shown in Figures 6a, 6b and 6c, respectively. First of all, it is interesting to verify that the RH values initially assessed in all specimens and depths of measurement were in the interval 97%-100%, indicating the capacity of the experimental setup to assess the elevated initial RH in the cementitious matrix. It was also observed that the decrease in RH values during the first 7 days in which the specimens were sealed was negligible, according to the expected behaviour for a high w/c concrete (w/c = 0.51), in which drying due to self-desiccation is known to be extremely low [14]. The observation of the humidity profiles in the deepest measurement point of each specimen (d3) allows concluding that the smallest sized specimen (S10) had almost reached full equilibrium with the RH = 60% of the surrounding environment at the age of 322 days, with recorded humidity of ~65%. Distinct situations were observed in S15 and S20 that registered RH values of 73% and 80%, respectively, for the same age of testing, and at the symmetry plane of drying (d3), which is a clear indication that the drying process was not near its conclusion yet.

A final comparison is presented in regard to the depths of measurement that were common to all specimens: 2 cm and 4 cm from the drying surface. Even though the results are relatively similar among the three sizes of specimens, there is a clear tendency for the thicker specimens to exhibit higher humidity values at similar depths in view of the transport of water that occurs from the core regions to the near surface regions. An example of such difference can be seen at the age of 322 days, in which the RH at 2 cm depth is of 62.9%, 64.5% and 66.0% for specimens S10, S15 and S20, respectively.

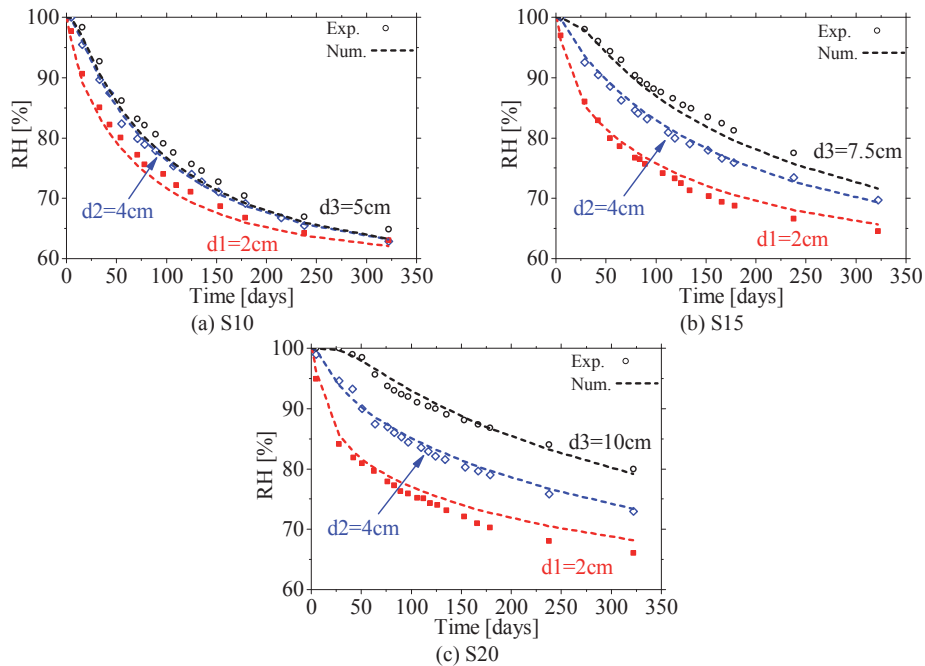


Figure 6: Measured humidity in specimens: (a) S10; (b) S15 and (c) S20: experimental and numerical predictions.

3.3 Humidity field simulations

The driving potential selected for simulating the moisture field is the average pore humidity, according to the reasons forwarded in [1]. The governing equation has strong affinities with the proposal for moisture diffusion of MC2010 [15]:

$$\frac{\partial RH}{\partial t} = \text{div}(D_{H^*} \cdot \text{grad}(RH)) \quad (1)$$

where RH is the relative humidity in the pores, t is the time (s), and D_{H^*} is the diffusivity. Due to the type of concrete tested (high w/c ratio), it was considered that the influence of self-desiccation in the pore humidity is negligible. The diffusion parameter D_{H^*} is modelled according to the following equation, initially forwarded by Bazant [16]:

$$D_{H^*} = D_1 \left[\alpha_H + \frac{1-\alpha_H}{1 + \left[\frac{1-RH}{1-RH_c} \right]^n} \right] \quad \text{with} \quad \alpha_H = \frac{D_0}{D_1} \quad (2)$$

Where D_1 and D_0 are, respectively, the values of D_{H^*} for $RH=1$ and $RH=0$, RH_c is the relative humidity for which $D_{H^*} = 0.5 \times D_1$, and n is a material property. In regard to the boundary conditions, a Neumann-type approach was followed:

$$q_m = h_m (RH_{surf} - RH_{env}) \quad (3)$$

Where q_m is the moisture flux flowing through the boundary, h_m is the moisture emissivity coefficient, and RH_{surf} and RH_{env} are, respectively, the values of RH on the surface and on the surrounding environment.

The parameters for the moisture model were obtained through back-analysis of the results of the monitoring process in the three concrete specimens S10, S15 and S20. The best solution was found with the following criteria: (i) the values of n and RH_c of Eq. (2) were established with basis on the results reported by Kim [14] and (ii) the values of h_m , D_1 and α_h in Eqs. (2) and (3) were determined in order to best-fit the experimental humidity curves obtained on the concrete specimens, ensuring that the order of magnitude is respected, according to the values reported by Kim [14] and on the MC2010 [15]. The resulting set of adopted parameters revealed a very good fit to the experimental data at all depths and times in the three types of studied concrete specimen geometries, as shown in Figure 7. This final set of parameters was: $n = 2$; $RH_c = 0.8$; $h_m = 4.81 \times 10^{-8} \text{ ms}^{-1}$; $D_1 = 3.08 \times 10^{-10} \text{ m}^2\text{s}^{-1}$; $\alpha_h = 0.0967$. Taking into account that this single set of parameters led to remarkable coherence between the numerical predictions and the experimentally observed values, it can be considered that the adopted strategy for humidity simulation is feasible and accurate.

4 Conclusions

From the experimental program reported in Section 2, targeted to evaluate experimental issues in measuring internal humidity of cement-based materials through embedded probes, the following main conclusions can be drawn:

- Among the 4 commercial sensors tested in this programme, there were no distinctive behavioural differences, indicating that all tested probes were adequate for the task;
- The presence of Gore-Tex fabric to protect the measuring sleeves during the casting process do not seem to negatively affect the quality of the measurements of humidity;
- The permanently installed sensors exhibited a similar behaviour to the discrete monitoring at specific instants by placing/removing probes from the measuring sleeve.

Furthermore, the additional experimental/numerical simulation programme allowed concluding that the approach of Model Code 1990/2010 can be applied with success to the simulation of humidity profiles measured by embedded humidity sensors. This validation is considered especially relevant in the sense that the same set of parameters allowed the simulation of moisture profiles in three distinct specimen sizes, monitored at three depths each.

Acknowledgments

This work was also financed by FEDER funds through the Competitiveness Operational Programme - COMPETE and by national funds through FCT within the scope of the projects POCI-01-0145-FEDER-007633 and POCI-01-0145-FEDER-016841 (IntegraCrete - PTDC/ECM-EST/1056/2014). The PhD grant of the second author is also gratefully acknowledged (SFRH/BD/80682/2011).

References

- [1] Azenha, M., et al., Thermo-hygro-mechanical modelling of self-induced stresses during the service life of RC structures, *Engineering Structures* 12 (2011), 3442-3453.
- [2] Chang, C.-Y. and Hung, S.-S., Implementing RFIC and sensor technology to measure temperature and humidity inside concrete structures, *Construction and Building Materials* 1 (2012), 628-637.
- [3] Ekaputri, J. J., et al., Internal relative humidity measurement on moisture distribution of mortar considering self-desiccation at early ages, Saitama, Japan (2010).
- [4] Grasley, Z. C., et al., Internal relative humidity and drying stress gradients in concrete, *Materials and Structures* 9 (2006), 901-909.
- [5] Vaisala, Humidity, dewpoint and temperature instruments, (1999), 2
- [6] Proceq, Hygropin - Operating Instructions - Moisture Meter, Switzerland (2012), 16
- [7] Sensirion, Datasheet SHT7x (SHT71, SHT75). Humidity and Temperature Sensor IC, (2011), 12
- [8] Honeywell, HIH-4000 Series Humidity Sensors, (2010), 6
- [9] Hansen, K. K., et al., Drying of concrete. Part I: A comparison of instruments for measuring the relative humidity in concrete structures, *Papers and Abstracts from the Third International Symposium on Humidity and Moisture*, Teddington, UK (1998), 279-287.
- [10] Granja, J. L., et al., Hygrometric Assessment of Internal Relative Humidity in Concrete: Practical Application Issues, *Journal of Advanced Concrete Technology* 8 (2014), 250-265.
- [11] Grasley, Z. C., Measuring and Modeling the Time-dependent Response of Cementitious Materials to Internal Stresses, University of Illinois (2002).
- [12] Dobrusskin, S., et al., Humidification with moisture permeable materials, Uppsala, Sweden (1991), 12
- [13] CEN, EN 206-1: Concrete: Specification, performance, production & conformity, (2000).
- [14] Kim, J. K. and Lee, C. S., Prediction of differential drying shrinkage in concrete, *Cement and Concrete Research* 7 (1998), 985-994.
- [15] Lin, S. K., et al., Use of the normalized impact-echo spectrum to monitor the setting process of mortar, *NDT and E International* 5 (2010), 385-393.
- [16] Bažant, Z. P. and Najjar, L. J., Nonlinear water diffusion in nonsaturated concrete, *Matériaux et Constructions* 1 (1972), 3-20.